Quantum Field Theory on a Highly Symmetric Lattice

Marco Aliberti

Università degli Studi di Torino

23rd October, 2023

The Strong Interaction

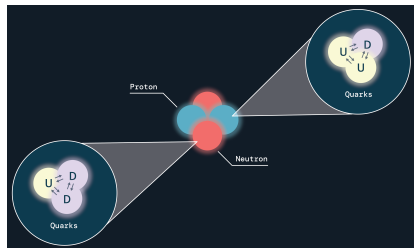Matter is made of   Atoms

Image credits: NASA[NASA, 2022]

The Strong Interaction

Matter is made of Atoms

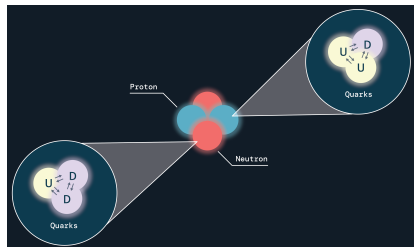Atoms are made of Nuclei and Electrons

Image credits: NASA[NASA, 2022]

The Strong Interaction

Matter is made of **Atoms**

Atoms are made of **Nuclei** and **Electrons**

Nuclei are made of Protons and Neutrons,

composed of **Quarks** and **Gluons**

Image credits: NASA[NASA, 2022]

The Strong Interaction

Matter is made of Atoms

Atoms are made of Nuclei and Electrons

Nuclei are made of Protons and Neutrons,
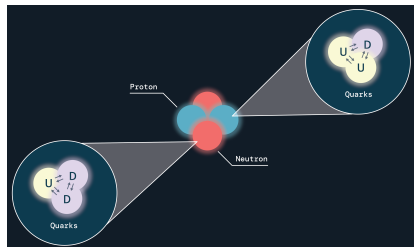composed of Quarks and Gluons

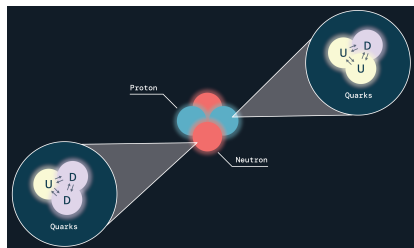Quarks and Gluons
Described by Quantum
Chromodynamics (QCD)

Image credits: NASA[NASA, 2022]

Quantum Chromodynamics (QCD)

Described by an $SU(3)$ Yang-Mills theory

$$S = \frac{1}{4} \int \mathrm{d}^4 x F^a_{\mu\nu}(x) F^{a\mu\nu}(x)$$

$$F^a_{\mu\nu} = \partial_\mu A^a_\nu - \partial_\nu A^a_\mu - g f^a_{bc} A^b_\mu A^c_\nu$$
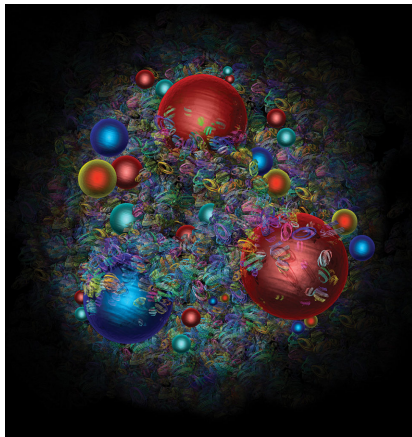

Figure: An artist's representation of a proton[CERN, 2019].

Quantum Chromodynamics (QCD)

Described by an $SU(3)$ Yang-Mills theory

$$S = \frac{1}{4} \int \mathrm{d}^4 x F_{\mu\nu}^a(x) F^{a\mu\nu}(x)$$

$$F_{\mu\nu}^a = \partial_\mu A_\nu^a - \partial_\nu A_\mu^a - g f_{bc}^a A_\mu^b A_\nu^c$$
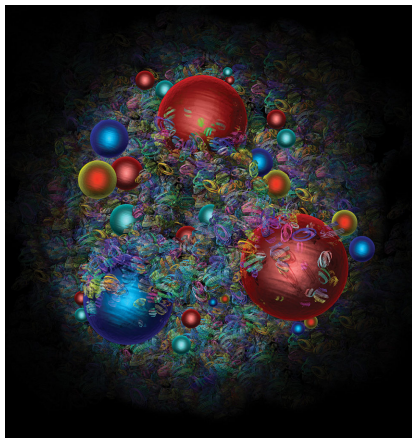
- 3 color charges

Figure: An artist's representation of a proton[CERN, 2019].

Quantum Chromodynamics (QCD)

Described by an $SU(3)$ Yang-Mills theory

$$S = \frac{1}{4} \int \mathrm{d}^4 x F_{\mu\nu}^a(x) F^{a\mu\nu}(x)$$

$$F_{\mu\nu}^a = \partial_\mu A_\nu^a - \partial_\nu A_\mu^a - g f_{bc}^a A_\mu^b A_\nu^c$$

- 3 color charges
- Interesting purely-gluonic physics

Figure: An artist's representation of a proton[CERN, 2019].

Quantum Chromodynamics (QCD)

Described by an $SU(3)$ Yang-Mills theory

$$S = \frac{1}{4} \int \mathrm{d}^4 x F_{\mu\nu}^a(x) F^{a\mu\nu}(x)$$

$$F_{\mu\nu}^a = \partial_\mu A_\nu^a - \partial_\nu A_\mu^a - g f_{bc}^a A_\mu^b A_\nu^c$$

- 3 color charges
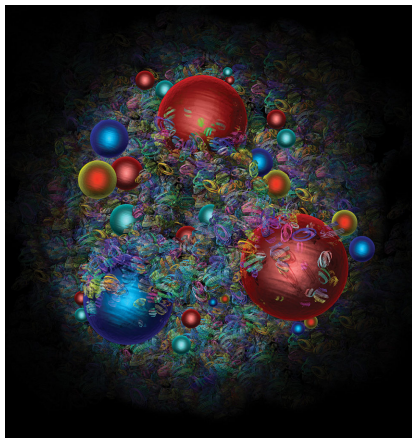- Interesting purely-gluonic physics
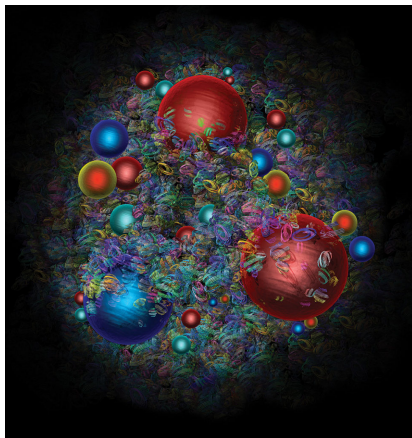- Heavily non-perturbative nature (except for specific regimes)

Figure: An artist's representation of a proton[CERN, 2019].

Quantum Chromodynamics (QCD)

Described by an $SU(3)$ Yang-Mills theory

$$S = \frac{1}{4} \int \mathrm{d}^4 x F^a_{\mu\nu}(x) F^{a\mu\nu}(x)$$

$$F^a_{\mu\nu} = \partial_\mu A^a_\nu - \partial_\nu A^a_\mu - g f^a_{bc} A^b_\mu A^c_\nu$$

- 3 color charges
- Interesting purely-gluonic physics
- Heavily non-perturbative nature (except for specific regimes)

$$\Downarrow$$

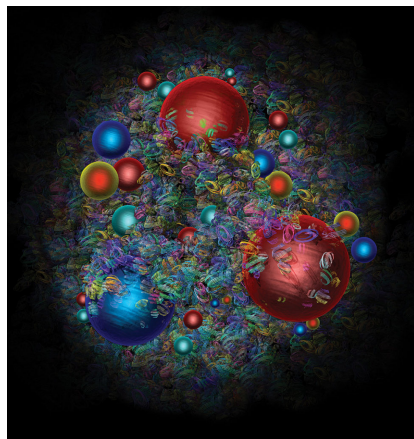Lattice Field Theory

Figure: An artist's representation of a proton[CERN, 2019].

What is a Lattice?

Definition: Lattice Λ

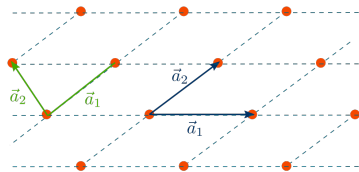$\Lambda = \{ \sum_{i=1}^{n} a_i e_i \mid a_i \in \mathbb{Z} \}$, with $\{e_i\}$ any basis of $\mathbb{R}^n$

Figure: A bidimensional lattice.

What is a Lattice?

Definition: Lattice Λ

$\Lambda = \left\{ \sum_{i=1}^{n} a_i e_i \mid a_i \in \mathbb{Z} \right\}$, with $\{e_i\}$ any basis of $\mathbb{R}^n$
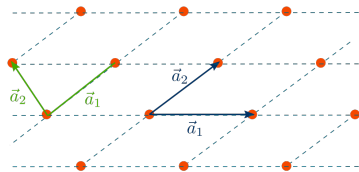

Figure: A bidimensional lattice.

Hypercubic lattice

$\{e_i\}$ is the canonical basis of $\mathbb{R}^n$
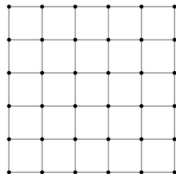a is called *lattice spacing*.

Figure: A square lattice.
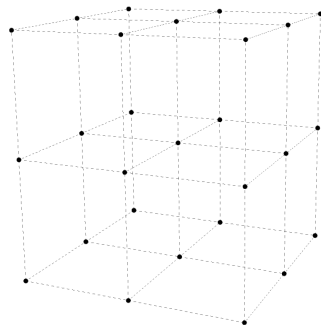
Lattice Field Theory

Basic idea

Fields can take values only in given parts of the lattice, $x \rightarrow n \in \Lambda$.

Figure: A (hyper)cubic lattice in $\mathbb{R}^3$.

Lattice Field Theory

Basic idea

Fields can take values only in given parts of the lattice, $x \to n \in \Lambda$.

Examples:

- Scalar fields $\Phi(x) \to \Phi(n)$ on sites

Figure: A (hyper)cubic lattice in $\mathbb{R}^3$.

Lattice Field Theory

Basic idea

Fields can take values only in given parts of the lattice, $x \rightarrow n \in \Lambda$.

Examples:

- Scalar fields $\Phi(x) \rightarrow \Phi(n)$ on sites
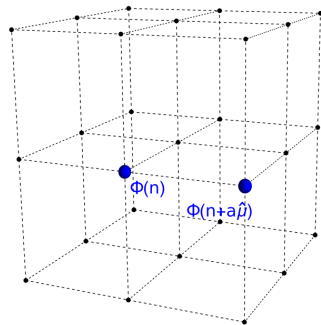- Vector fields $U_\mu(x) \rightarrow U_\mu(n)$ on links
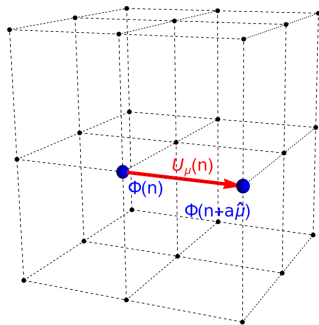
Parallel Transporter

$$U_\mu(x) = \exp(igaA_\mu(x))$$

Figure: A (hyper)cubic lattice in $\mathbb{R}^3$.

Lattice Field Theory

Basic idea

Fields can take values only in given parts of the lattice, $x \to n \in \Lambda$.

Examples:

- Scalar fields $\Phi(x) \to \Phi(n)$ on sites
- Vector fields $U_\mu(x) \to U_\mu(n)$ on links
- Object with k indices on k-symplexes
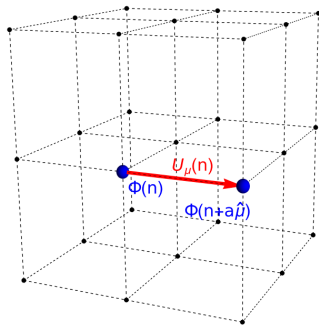
Parallel Transporter

$$U_\mu(x) = \exp(igaA_\mu(x))$$

Figure: A (hyper)cubic lattice in $\mathbb{R}^3$.

Lattice Field Theory

Basic idea
Fields can take values only in given parts of the lattice, $x \rightarrow n \in \Lambda$.

Examples:

- Scalar fields $\Phi(x) \rightarrow \Phi(n)$ on sites
- Vector fields $U_\mu(x) \rightarrow U_\mu(n)$ on links
- Object with k indices on k-symplexes

Beware!
Spinorial fields are trickier to be discretized.

Parallel Transporter
$$U_\mu(x) = \exp(igaA_\mu(x))$$
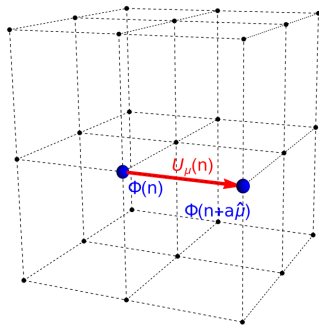

$U_\mu(n)$

$\Phi(n)$

$\Phi(n+a\hat{\mu})$

Figure: A (hyper)cubic lattice in $\mathbb{R}^3$.

Gauge-Invariant Observables and Wilson Action

The Yang-Mills continuum action is
$S_E = \frac{1}{4} \int \mathrm{d}^4 x F^{a\mu\nu}(x) F^a_{\mu\nu}(x)$.

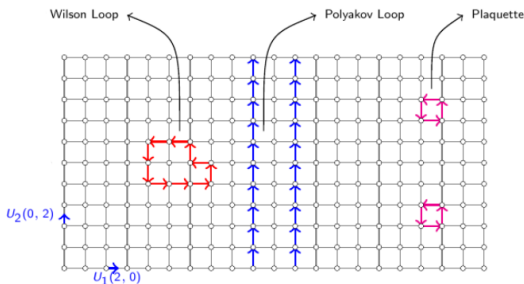On the lattice, every closed path is gauge-invariant.

Figure: Gauge-invariant paths on a bidimensional lattice[Sigdel, 2016].

Gauge-Invariant Observables and Wilson Action

The Yang-Mills continuum action is
$S_E = \frac{1}{4} \int \mathrm{d}^4 x \, F^{a\mu\nu}(x) F^a_{\mu\nu}(x)$.

On the lattice, every closed path is gauge-invariant.

Definition: Plaquette $U_{\mu\nu}(n)$

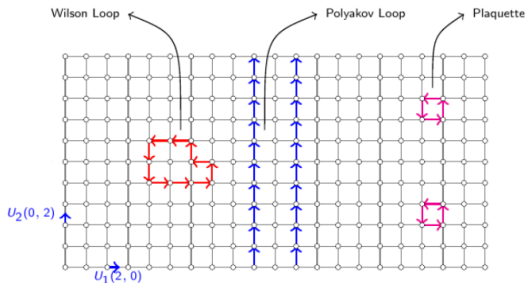$U_\mu(n) U_\nu(n+\mu) U_\mu^\dagger(n+\nu) U_\nu^\dagger(n)$

Figure: Gauge-invariant paths on a bidimensional lattice[Sigdel, 2016].

Gauge-Invariant Observables and Wilson Action

The Yang-Mills continuum action is
$S_E = \frac{1}{4} \int \mathrm{d}^4 x\, F^{a\mu\nu}(x) F^a_{\mu\nu}(x)$.

On the lattice, every closed path is gauge-invariant.

Definition: Plaquette $U_{\mu\nu}(n)$

$U_\mu(n) U_\nu(n+\mu) U_\mu^\dagger(n+\nu) U_\nu^\dagger(n)$

Wilson's Idea

$S = \frac{\beta}{2N} \sum_{n,\mu,\nu} \mathfrak{Re}\, \mathrm{Tr}\, (\mathbb{1} - U_{\mu\nu}(n))$
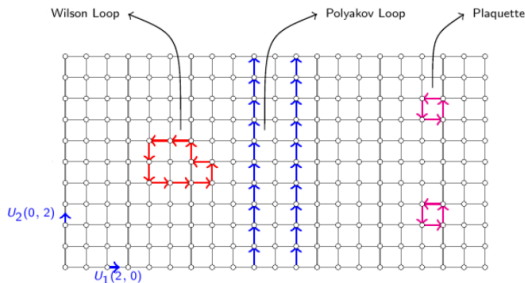

Figure: Gauge-invariant paths on a bidimensional lattice[Sigdel, 2016].

Polyakov Loops and Potential

If the time coordinate is taken to be
periodic, more closed paths arise.

Polyakov Loop

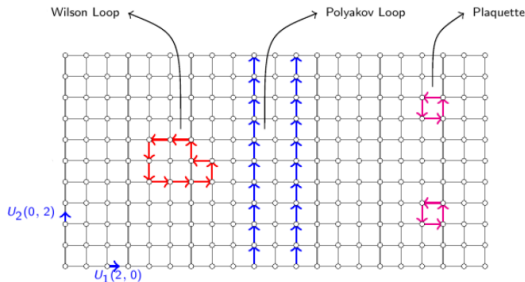$$P(n) = \text{Tr} \prod_{t=0}^{T-1} U_t(n)$$

Figure: Gauge-invariant paths on a bidimensional lattice[Sigdel, 2016].

Polyakov Loops and Potential

If the time coordinate is taken to be periodic, more closed paths arise.

The expectation value of two Polyakov loops is the potential.

Polyakov Loop

$$P(n) = \text{Tr} \prod_{t=0}^{T-1} U_t(n)$$

Potential

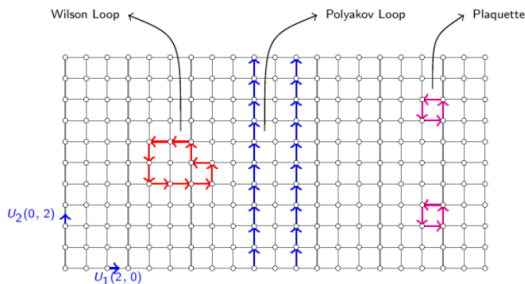$$V(R) = -\frac{1}{T} \log < P(0) P^\dagger(R) >$$

Figure: Gauge-invariant paths on a bidimensional lattice[Sigdel, 2016].

Monte Carlo Simulations

Computers are used to simulate Lattice Field Theories

Figure: A rendering of the CINECA Leonardo supercomputer[Wikipedia, 2022].

Monte Carlo Simulations

Computers are used to simulate Lattice Field Theories

- Random configurations of link variables are generated.

Figure: A rendering of the CINECA Leonardo supercomputer[Wikipedia, 2022].

Monte Carlo Simulations

Computers are used to simulate Lattice Field Theories

- Random configurations of link variables are generated.
- Proper Monte Carlo algorithms evolve the configurations towards minimums of the action.

Figure: A rendering of the CINECA Leonardo supercomputer[Wikipedia, 2022].

Monte Carlo Simulations

Computers are used to simulate Lattice Field Theories

- Random configurations of link variables are generated.
- Proper Monte Carlo algorithms evolve the configurations towards minimums of the action.
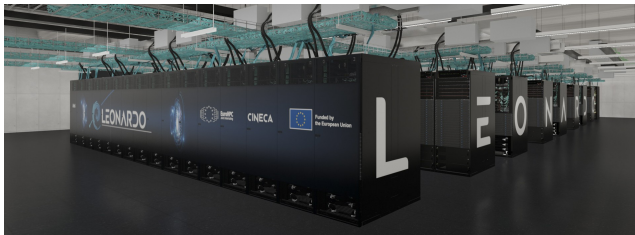- A great number of observables is evaluated and then their mean value is computed.

Figure: A rendering of the CINECA Leonardo supercomputer[Wikipedia, 2022].

Lattice Symmetries

Poincaré Group can be divided in:

Translations

Rotations

Lattice Symmetries

Poincaré Group can be divided in:

Translations

$$x^\mu \to x^\mu + \varepsilon^\mu$$
$$\Downarrow$$
$$n \to n + a\hat{\mu}$$

Rotations

Lattice Symmetries

Poincaré Group can be divided in:

Translations

$$x^\mu \to x^\mu + \varepsilon^\mu$$

$$\Downarrow$$

$$n \to n + a\hat{\mu}$$

Rotations

$$x^\mu \to R^\mu_\nu x^\nu \quad R \in SO(4)$$

$$\Downarrow$$

$$n \to \Gamma n \quad \Gamma \in G_{\Lambda_{SH}}$$

$G_{\Lambda_{SH}}$: group of rotations of multiples of $90°$ around any axis.

Lattice Symmetries

Poincaré Group can be divided in:

Translations
$x^\mu \rightarrow x^\mu + \varepsilon^\mu$
$\Downarrow$
$n \rightarrow n + a\hat{\mu}$

Rotations
$x^\mu \rightarrow R^\mu_\nu x^\nu \quad R \in SO(4)$
$\Downarrow$
$n \rightarrow \Gamma n \quad \Gamma \in G_{\Lambda_{SH}}$

$G_{\Lambda_{SH}}$: group of rotations of multiples of $90°$ around any axis.

$a\hat{\mu} \rightarrow \varepsilon^\mu$ for $a \rightarrow 0$

Poincaré Group can be divided in:

Translations
$x^\mu \to x^\mu + \varepsilon^\mu$
$\Downarrow$
$n \to n + a\hat{\mu}$

Rotations
$x^\mu \to R_\nu^\mu x^\nu \quad R \in SO(4)$
$\Downarrow$
$n \to \Gamma n \quad \Gamma \in G_{\Lambda_{SH}}$

$G_{\Lambda_{SH}}$: group of rotations of multiples of $90°$ around any axis.

$a\hat{\mu} \to \varepsilon^\mu$ for $a \to 0$

$\Gamma \not\to R$ for $a \to 0$

Lattice Symmetries

Poincaré Group can be divided in:

Translations

$$x^\mu \to x^\mu + \varepsilon^\mu$$
$$\Downarrow$$
$$n \to n + a\hat{\mu}$$

Rotations

$$x^\mu \to R^\mu_\nu x^\nu \quad R \in SO(4)$$
$$\Downarrow$$
$$n \to \Gamma n \quad \Gamma \in G_{\Lambda_{SH}}$$

$G_{\Lambda_{SH}}$: group of rotations of multiples of $90°$ around any axis.

$a\hat{\mu} \to \varepsilon^\mu$ for $a \to 0$

$\Gamma \not\to R$ for $a \to 0$

Important:

Rotational invariance seems to be broken.

Equipotential surfaces become spheres as the continuum limit is approached[Lang and Rebbi, 1982].

The gauge group used was the discrete icosahedral subgroup $\tilde{Y} \subset SU(2)$.

(a)   (b)
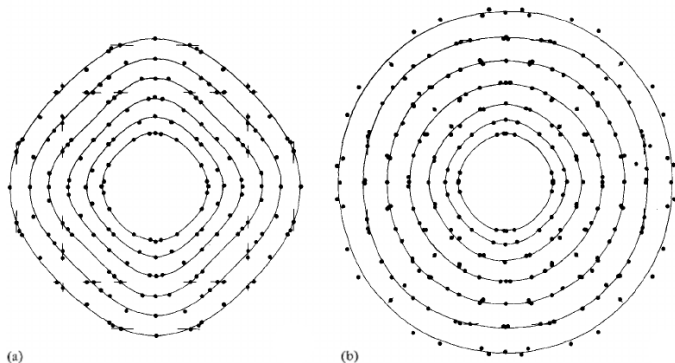
Figure: Restoration of rotational invariance from (a) $\beta = 2$, $n_s = 8$, $n_t = 4$ to (b) $\beta = 2.25$, $n_s = 16$, $n_t = 6$; the curves represent equipotential curves.

Rotational Invariance Restoration

Results of simulations for gauge group $SU(2)$ with 20000 measurements each[1]. Approach slightly different than Lang and Rebbi's.
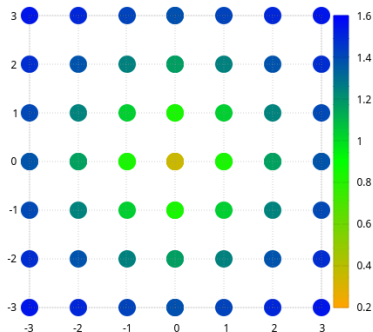
Figure: Potential from $\beta = 2.20$, $n_s = 8$, $n_t = 4$.
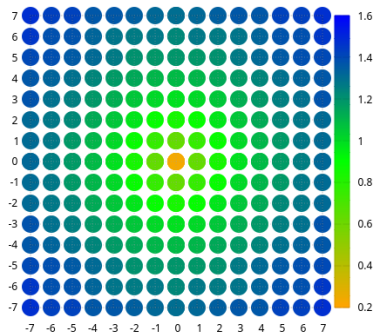
Figure: Potential from $\beta = 2.35$, $n_s = 16$, $n_t = 6$.

[1]The simulation code is based on the code presented in refs. [Panero, 2009; Mykkänen, Panero, and Rummukainen, 2012].

Higher Symmetry Lattices

Other, more rotational-symmetric, lattices have been used:

Body Centered Tesseract
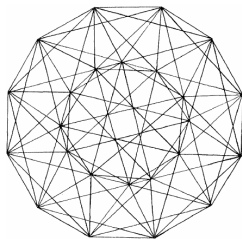
- 24 nearest neighbours
- 1152-element symmetry group
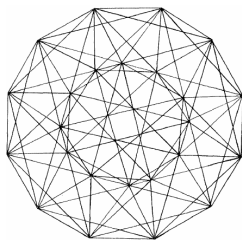
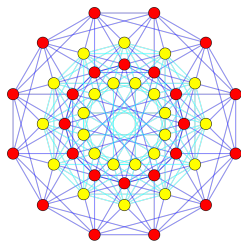Figure: Two-dimensional projection of
a BCT[Celmaster, 1982].

The SH lattice has 8 nearest neighbours and a 384-element symmetry group.

Higher Symmetry Lattices

Other, more rotational-symmetric, lattices have been used:

Body Centered Tesseract
- 24 nearest neighbours
- 1152-element symmetry group

F_4 coroots lattice[Neuberger, 1987]
- 48 nearest neighbours
- 2304-element symmetry group

Figure: Two-dimensional projection of a BCT[Celmaster, 1982].

Figure: Two-dimensional projection of a F_4 coroots lattice[Wikipedia, 2010].

The SH lattice has 8 nearest neighbours and a 384-element symmetry group.

➤ Obtained from Simple Hypercubic lattice considering also the centers;
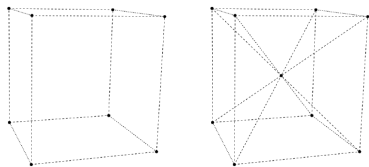
Figure: Cubic Cell (left) and BC Cubic Cell (right).

➤ Obtained from Simple Hypercubic lattice considering also the centers;
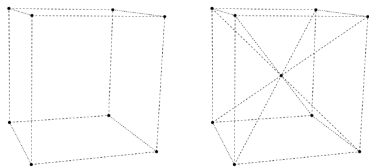
➤ Elementary cell is the 24-cell;

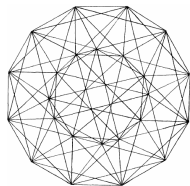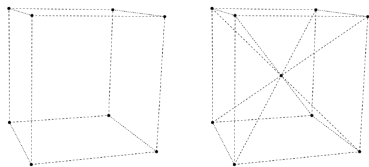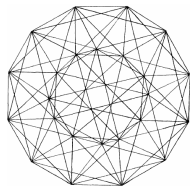Figure: Cubic Cell (left) and BC Cubic Cell (right).

Figure: Bidimensional projection of the 24-cell.

Body Centered Tesseract (BCT)

➤ Obtained from Simple Hypercubic lattice considering also the centers;

➤ Elementary cell is the 24-cell;

➤ Has 24 nearest neighbours:
  - The 8 possible permutations of $(\pm 1, 0, 0, 0)$
  - The 16 vectors of the form $\left(\pm\frac{1}{2}, \pm\frac{1}{2}, \pm\frac{1}{2}, \pm\frac{1}{2}\right)$
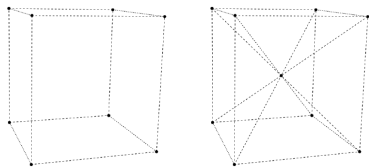

Figure: Cubic Cell (left) and BC Cubic Cell (right).

Figure: Bidimensional projection of the 24-cell.

Body Centered Tesseract (BCT)

➤ Obtained from Simple Hypercubic lattice considering also the centers;

➤ Elementary cell is the 24-cell;

➤ Has 24 nearest neighbours:
- The 8 possible permutations of $(\pm 1, 0, 0, 0)$
- The 16 vectors of the form $\left(\pm\frac{1}{2}, \pm\frac{1}{2}, \pm\frac{1}{2}, \pm\frac{1}{2}\right)$

➤ Plaquettes are triangular;

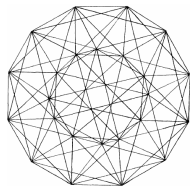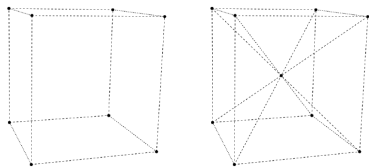Figure: Cubic Cell (left) and BC Cubic Cell (right).

Figure: Bidimensional projection of the 24-cell.

Body Centered Tesseract (BCT)

➤ Obtained from Simple Hypercubic lattice considering also the centers;

➤ Elementary cell is the 24-cell;

➤ Has 24 nearest neighbours:
  - The 8 possible permutations of $(\pm 1, 0, 0, 0)$
  - The 16 vectors of the form $\left(\pm\frac{1}{2}, \pm\frac{1}{2}, \pm\frac{1}{2}, \pm\frac{1}{2}\right)$

➤ Plaquettes are triangular;

➤ Contains the Simple Hypercubic lattice;

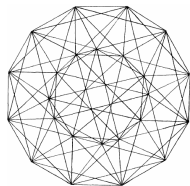Figure: Cubic Cell (left) and BC Cubic Cell (right).

Figure: Bidimensional projection of the 24-cell.

Body Centered Tesseract (BCT)

- ➤ Obtained from Simple Hypercubic lattice considering also the centers;
- ➤ Elementary cell is the 24-cell;
- ➤ Has 24 nearest neighbours:
  - The 8 possible permutations of $(\pm 1, 0, 0, 0)$
  - The 16 vectors of the form $\left(\pm\frac{1}{2}, \pm\frac{1}{2}, \pm\frac{1}{2}, \pm\frac{1}{2}\right)$
- ➤ Plaquettes are triangular;
- ➤ Contains the Simple Hypercubic lattice;
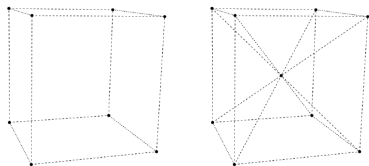- ➤ Has been used to simulate $SU(2)$ Yang-Mills theories, in [Celmaster, 1982].

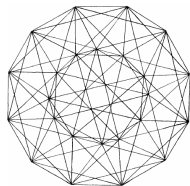Figure: Cubic Cell (left) and BC Cubic Cell (right).

Figure: Bidimensional projection of the 24-cell.

F_4 Coroots Lattice

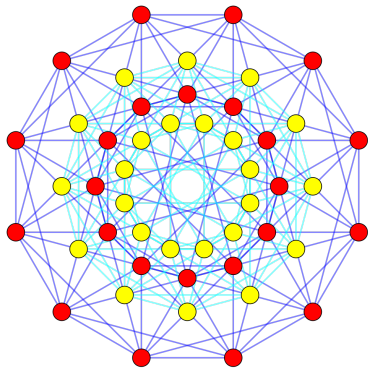➤ Obtained from the roots lattice of the exceptional Lie algebra F_4 and its dual;

Figure: Bidimensional projection of the F_4 lattice.

F_4 Coroots Lattice

➤ Obtained from the roots lattice of the exceptional Lie algebra F_4 and its dual;

➤ Has 48 nearest neighbours:

  • The 24 roots are all possible permutations of coordinate positions of $(\pm 1, \pm 1, 0, 0)$
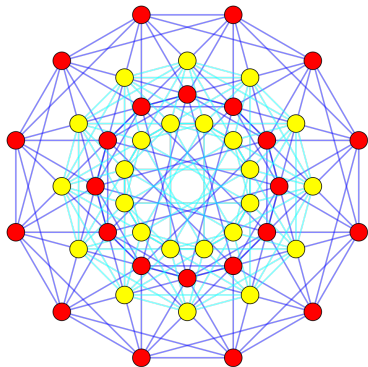

Figure: The 24 roots (red) of the F_4 lattice, projected on a bidimensional plane.

F_4 Coroots Lattice

➤ Obtained from the roots lattice of the exceptional Lie algebra F_4 and its dual;

➤ Has 48 nearest neighbours:

- The 24 roots are all possible permutations of coordinate positions of $(\pm 1, \pm 1, 0, 0)$
- The 24 dual roots (coroots) are:
  - ❍ The 8 possible permutations of $(\pm 1, 0, 0, 0)$
  - ❍ The 16 vectors of the form $\left(\pm \frac{1}{2}, \pm \frac{1}{2}, \pm \frac{1}{2}, \pm \frac{1}{2}\right)$
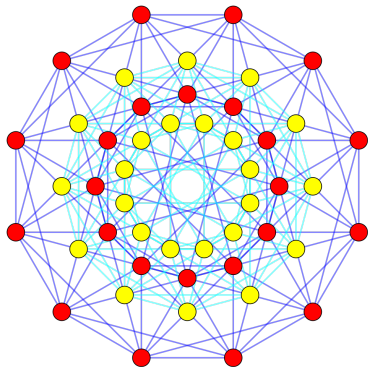

Figure: The 24 roots (red) and the 24 coroots (yellow) of the F_4 lattice, projected on a bidimensional plane.

F_4 Coroots Lattice

➤ Obtained from the roots lattice of the exceptional Lie algebra F_4 and its dual;

➤ Has 48 nearest neighbours:

- The 24 roots are all possible permutations of coordinate positions of $(\pm 1, \pm 1, 0, 0)$
- The 24 dual roots (coroots) are:
  - ❍ The 8 possible permutations of $(\pm 1, 0, 0, 0)$
  - ❍ The 16 vectors of the form $\left(\pm\frac{1}{2}, \pm\frac{1}{2}, \pm\frac{1}{2}, \pm\frac{1}{2}\right)$

➤ Exists only in 4 dimensions;

Figure: The 24 roots (red) and the 24 coroots (yellow) of the F_4 lattice, projected on a bidimensional plane.

F_4 Coroots Lattice

➤ Obtained from the roots lattice of the exceptional Lie algebra F_4 and its dual;

➤ Has 48 nearest neighbours:

- The 24 roots are all possible permutations of coordinate positions of $(\pm 1, \pm 1, 0, 0)$
- The 24 dual roots (coroots) are:
  - ❍ The 8 possible permutations of $(\pm 1, 0, 0, 0)$
  - ❍ The 16 vectors of the form $(\pm\frac{1}{2}, \pm\frac{1}{2}, \pm\frac{1}{2}, \pm\frac{1}{2})$
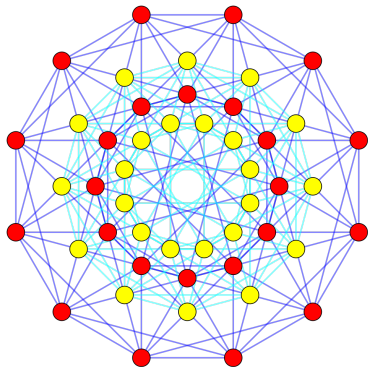
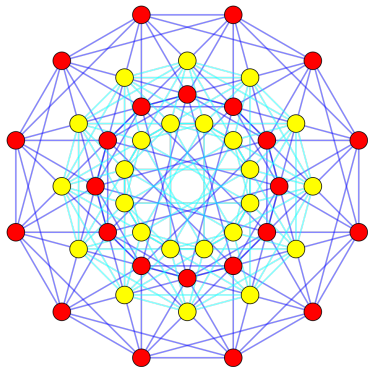➤ Exists only in 4 dimensions;

➤ Is a more symmetric version of the BCT;

Figure: The 24 roots (red) and the 24 coroots (yellow) of the F_4 lattice, projected on a bidimensional plane.

F_4 Coroots Lattice

➤ Obtained from the roots lattice of the exceptional Lie algebra F_4 and its dual;

➤ Has 48 nearest neighbours:
  - The 24 roots are all possible permutations of coordinate positions of $(\pm 1, \pm 1, 0, 0)$
  - The 24 dual roots (coroots) are:
    ○ The 8 possible permutations of $(\pm 1, 0, 0, 0)$
    ○ The 16 vectors of the form $(\pm\frac{1}{2}, \pm\frac{1}{2}, \pm\frac{1}{2}, \pm\frac{1}{2})$

➤ Exists only in 4 dimensions;

➤ Is a more symmetric version of the BCT;

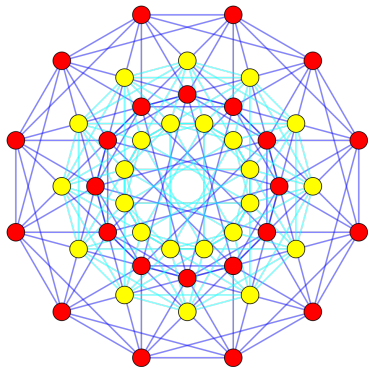➤ Has been used only to simulate scalar fields, in [Neuberger, 1987].

Figure: The 24 roots (red) and the 24 coroots (yellow) of the F_4 lattice, projected on a bidimensional plane.
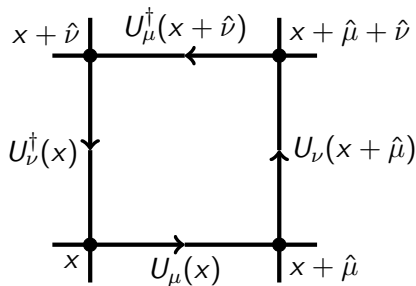
Simulations on SH Lattice

Wilson Action:

$$S_W = \frac{\beta}{2N} \sum_{x \in \Lambda} \sum_{\mu < \nu} \Re\mathfrak{e} \, \text{Tr}[\mathbb{1} - U_{\mu\nu}(x)]$$

Plaquette:

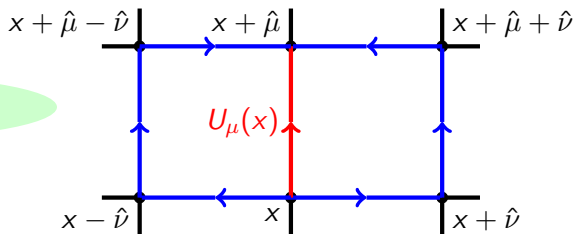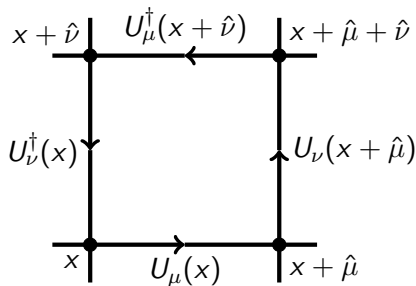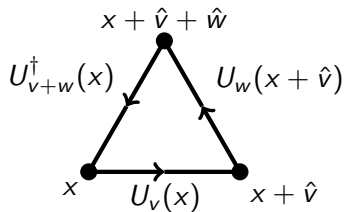$$U_{\mu\nu} = U_\mu(x) U_\nu(x + \hat{\mu}) U_\mu^\dagger(x + \hat{\nu}) U_\nu^\dagger(x)$$

Simulations on SH Lattice

Wilson Action:

$$S_W = \frac{\beta}{2N} \sum_{x \in \Lambda} \sum_{\mu < \nu} \mathfrak{Re} \, \mathrm{Tr}[\mathbb{1} - U_{\mu\nu}(x)]$$

Plaquette:

$$U_{\mu\nu} = U_\mu(x) U_\nu(x + \hat\mu) U_\mu^\dagger(x + \hat\nu) U_\nu^\dagger(x)$$

6 staples for each link

BCT Action:

$$S_{BCT} = \frac{\beta}{8} \sum_{\triangle} \mathfrak{Re}\, \mathsf{Tr}\, U_{\triangle}$$

Plaquette:

$$U_{\triangle} = U_v(x) U_w(x + \hat{v}) U_{v+w}^{\dagger}(x)$$

BCT Action:

$$S_{BCT} = \frac{\beta}{8} \sum_\triangle \mathfrak{Re} \, \text{Tr} \, U_\triangle$$

Plaquette:

$$U_\triangle = {\color{red}U_v(x)}{\color{blue}U_w(x+\hat{v})}U_{v+w}^\dagger(x)$$
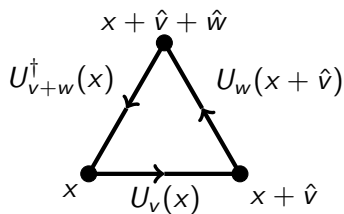
8 staples for each link
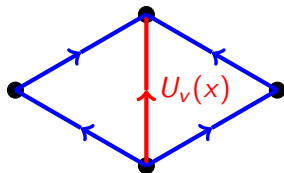
Thank you for your attention

Bibliography I

📄 NASA (2022). URL:
https://universe.nasa.gov/resources/254/strong-force/
(visited on 12/20/2022).

📄 CERN (2019). URL:
https://home.cern/news/news/physics/proton-century (visited
on 06/12/2019).

📄 Sigdel, Dibakar (2016). "Two Dimensional Lattice Gauge Theory with
and without Fermion Content". In: *FIU Electronic Theses and
Dissertations* 3224. DOI: 10.25148/etd.FIDC001748. URL:
https://digitalcommons.fiu.edu/etd/3224?utm_source=
digitalcommons.fiu.edu%2Fetd%2F3224&utm_medium=PDF&utm_
campaign=PDFCoverPages.

📄 Wikipedia (2022). URL: https://en.wikipedia.org/wiki/
Leonardo_(supercomputer)#/media/File:Modello_Leonardo.jpg
(visited on 09/25/2022).

Bibliography II

📄 Lang, C. B. and C. Rebbi (1982). "Potential and Restoration of Rotational Symmetry in SU(2) Lattice Gauge Theory". In: *Phys. Lett. B115.* [, 322 (1982)], p. 137. DOI: 10.1016/0370-2693(82)90813-9.

📄 Panero, Marco (2009). "Thermodynamics of the QCD plasma and the large-N limit". In: *Phys. Rev. Lett.* 103, p. 232001. DOI: 10.1103/PhysRevLett.103.232001. arXiv: 0907.3719 [hep-lat].

📄 Mykkänen, Anne, Marco Panero, and Kari Rummukainen (2012). "Casimir scaling and renormalization of Polyakov loops in large-N gauge theories". In: *JHEP* 1205, p. 069. DOI: 10.1007/JHEP05(2012)069. arXiv: 1202.2762 [hep-lat].

📄 Celmaster, William (1982). "Gauge Theories on the Body - Centered Hypercubic Lattice". In: *Phys. Rev.* D26, p. 2955. DOI: 10.1103/PhysRevD.26.2955.

📄 Neuberger, Herbert (1987). "SPINLESS FIELDS ON F(4) LATTICES". In: *Phys. Lett. B* 199, pp. 536–540. DOI: 10.1016/0370-2693(87)91623-6.

📄 Wikipedia (2010). URL: https://en.wikipedia.org/wiki/F4_%28mathematics%29#/media/File:F4_roots_by_24-cell_duals.svg (visited on 12/13/2010).